

## **Li<sub>6</sub>Zr<sub>2</sub>O<sub>7</sub>, a New Anion Vacancy ccp Based Structure, Determined by ab initio Powder Diffraction Methods**

I. ABRAHAM\*†

*Department of Chemistry, Queen Mary and Westfield College, University of London, Mile End Road, London E1 4NS, United Kingdom*

AND P. LIGHTFOOT AND P. G. BRUCE

*Centre for Electrochemical and Materials Sciences (CEMS), Department of Chemistry, University of St. Andrews, St. Andrews, Fife KY16 9ST, United Kingdom*

Received June 1, 1992; in revised form November 13, 1992; accepted November 16, 1992

The structure of Li<sub>6</sub>Zr<sub>2</sub>O<sub>7</sub>, Fw 336.08, has been determined ab initio using Patterson methods on X-ray powder diffraction data and refined using a combination of powder X-ray and neutron diffraction data. Li<sub>6</sub>Zr<sub>2</sub>O<sub>7</sub> crystallizes in the monoclinic space group C2/c with  $a = 10.4428(1)$ ,  $b = 5.9877(1)$ ,  $c = 10.2014(1)\text{\AA}$ ,  $\beta = 100.266(1)^\circ$ ,  $V = 627.67(1)\text{\AA}^3$ ,  $Z = 4$ , and  $D_c = 3.56\text{ g cm}^{-3}$ . The structure is based on a distorted ccp oxygen array with  $\frac{1}{4}$  of the oxygens missing. Zr and Li adopt a rock salt distribution with Zr in six-coordinate sites but with Li in five-coordinate square pyramidal sites arising from the anion vacancy. The Zr octahedra are arranged in edge-sharing pairs which corner-share with other pairs to give the three-dimensional structure. The lithium square-based pyramids which share edges with the Zr octahedra are arranged in clusters around the anion vacancy. The structure possesses some similarity to the hcp-based ramsdellite structure; the two structures are compared. The final  $R$  factors for the combined refinement are  $R_{wp} = 10.76\%$ ,  $R_{ex} = 5.01\%$ ,  $\chi^2 = 4.60$  for 53 basic variables with 11,895 observations, corresponding to 535 X-ray and 1264 neutron reflections. © 1993 Academic Press, Inc.

### **Introduction**

The Li<sub>2</sub>O–ZrO<sub>2</sub> system has been studied by a number of workers in recent years. Some compounds formed within this system have been investigated because of their properties as solid electrolytes (1, 2), whereas others have found quite different applications as linings for fusion reactors (3–5). The slow solid state reaction between

refractory ZrO<sub>2</sub> and volatile Li<sub>2</sub>O at elevated temperatures can lead to lithia loss, especially in materials with a high lithia content. As a result, lithium zirconates can be particularly difficult to prepare in pure form. Despite these problems, a variety of compositions have been identified and their crystal structures characterized, including Li<sub>2</sub>ZrO<sub>3</sub> (6) and Li<sub>8</sub>ZrO<sub>6</sub> (7).

Phases with the stoichiometry Li<sub>4</sub>ZrO<sub>4</sub> have been reported by a number of workers (8–10). In an extensive study of these systems, Enriquez *et al.* (11) reported the existence of two polymorphs of Li<sub>4</sub>ZrO<sub>4</sub>, obtainable from reaction mixtures containing 67 mole% in Li<sub>2</sub>CO<sub>3</sub>, which they desig-

\*Author to whom correspondence should be addressed.

† Previous address: Department of Chemistry, Heriot-Watt University, Riccarton, Edinburgh EH14 4AS, United Kingdom.

nated  $\alpha$  and  $\beta$ . X-ray powder diffraction data for the  $\alpha$  form, which was quenched from 900°C, were in agreement with the previously established powder diffraction pattern for  $\text{Li}_4\text{ZrO}_4$  (12). However, subsequently this powder pattern has been reassigned to a more lithium-deficient phase,  $\text{Li}_6\text{Zr}_2\text{O}_7$  (13, 14). The  $\beta$  material, which was obtained by quenching from 1400°C, showed a different diffraction pattern. In addition, Enriquez *et al.* also identified a metastable form of  $\text{Li}_6\text{Zr}_2\text{O}_7$ , which was prepared by quenching a mixture containing 60 mole%  $\text{Li}_2\text{CO}_3$  from temperatures between 600 and 750°C.

We have prepared a sample of  $\text{Li}_6\text{Zr}_2\text{O}_7$  with a powder pattern corresponding to that which had previously been attributed to  $\text{Li}_4\text{ZrO}_4$ . In the absence of any obvious structural analogues, ab initio techniques of structure determination offer a route by which the crystal structure may be elucidated. The structure solution of  $\text{Li}_6\text{Zr}_2\text{O}_7$  represents an ideal problem for heavy atom methods of structure determination because of the dominant X-ray scattering of Zr in this system. However, the weak scattering of X-rays by lithium makes it difficult to obtain accurate parameters for this ion from X-rays alone. Here we report the ab initio crystal structure determination of  $\text{Li}_6\text{Zr}_2\text{O}_7$  using powder X-ray data and its refinement using a combination of X-ray and neutron powder diffraction techniques.

## Experimental

### Preparation

$\text{Li}_6\text{Zr}_2\text{O}_7$  was prepared by solid state reaction between  $\text{Li}_2\text{CO}_3$  and  $\text{ZrO}_2$ . An appropriate quantity of  $\text{ZrO}_2$  was mixed with excess  $\text{Li}_2\text{CO}_3$  ( $^7\text{Li}_2\text{CO}_3$  for neutron diffraction samples) and ground as a slurry in ethanol for 15 min. The dried powder was placed in a gold boat and heated in a muffle furnace at 650°C for 6 hr followed by 24 hr at 900°C. The final product was quenched rapidly in liquid nitrogen. Weight

loss measurements confirmed loss of the excess  $\text{Li}_2\text{O}$ .

### Data Collection

X-ray powder diffraction data were collected on a Stoe STADI/P high resolution diffractometer in symmetric transmission mode using Ge-monochromatized  $\text{CuK}\alpha_1$  radiation. Data were collected in the  $2\theta$  range 10°–120° in steps of 0.02°, using a small linear position-sensitive detector. Calibration was with an external Si standard. No absorption correction was applied.

Time-of-flight powder neutron diffraction data were collected on the HRPD diffractometer at ISIS, Rutherford Appleton Laboratory. Approximately 10 g of finely ground material were placed in a 12 mm diameter vanadium can 1 m in front of the backscattering detectors. Data were collected in the time-of-flight range 30–230 ms at 298 K, with only the data between 30 and 102 ms used in refinement.

Data were fitted by a combined Rietveld method using the program GSAS (15), with peak shapes modeled by a convolution of a Gaussian and two exponential functions (16) in the case of the neutron data and a pseudo-Voigt function for the X-ray data. The neutron scattering lengths used were  $^7\text{Li} = -0.220$ ,  $\text{O} = 0.5805$ , and  $\text{Zr} = 0.716 \times 10^{-12}$  cm (17). Scattering curves for neutral atoms (18) were used in the X-ray refinement. Structural projections were generated using STRUPLO (19) and PLUTO (20).

### Structure Determination

Automatic indexing of the X-ray powder pattern using the program TREOR (21) confirmed the monoclinic cell previously reported (13). Systematic absences in the reflection data indicated that the likely space groups were  $Cc$  or  $C2/c$  (Nos. 9 and 15, respectively). The centrosymmetric option  $C2/c$  was assumed for subsequent data analysis. Extraction of integrated intensities from the X-ray data was carried out by the

method described by Le Bail *et al.* (22), which fits the whole pattern without a structural model, but allowing the usual profile and lattice parameters to vary. One hundred ninety-three reflections were extracted in the range  $5^\circ$ – $80^\circ$   $2\theta$ . These were used to generate a Patterson map, from which the position of the Zr atom was clearly evident. This atom was then used as input to a Rietveld refinement of the full data set ( $10^\circ$ – $130^\circ$   $2\theta$ , 535 reflections). After refinement of the Zr atomic coordinates, a difference Fourier synthesis revealed the positions of the four oxygen atoms as the strongest peaks. Subsequent refinement of these positions, followed by a further difference Fourier synthesis, revealed three probable Li positions. These were then introduced into the refinement, which proceeded with all atomic and profile parameters varying. No further atoms were evident in subsequent difference Fourier analyses.

The dominance of the heavy atom in the X-ray scattering was reflected in the relatively poor esd's obtained for the atomic parameters of the lighter atoms. In order to improve the accuracy and precision of these parameters, a high resolution powder neutron diffraction data set was introduced into a combined refinement with the original

X-ray data. For each data set, scale, peak shape, and five polynomial background parameters were refined individually with lattice, atomic, and thermal parameters refined in combination. In the final refinement isotropic thermal parameters were refined for all atoms. The final combined refinement terminated with  $R_{\text{wp}} = 10.76\%$ ,  $R_{\text{ex}} = 5.01\%$ , and  $\chi^2 = 4.60$  for 53 basic variables with 11,895 observations, corresponding to 535 X-ray and 1264 neutron reflections. The final parameters from the combined refinement are shown in Table I with significant contact distances in Table II.

### Discussion

The structure of  $\text{Li}_6\text{Zr}_2\text{O}_7$  is based on a distorted ccp oxide ion array with  $\frac{1}{8}$  of the oxygens missing. Zr and Li adopt an ordered rock salt distribution in the lattice, with Zr in six-coordinate octahedral geometry, but Li ions in five-coordinate square pyramidal sites. The square pyramidal sites arise from the vacancy in the anion lattice and correspond to five apexes of an octahedral site in a full ccp array.

The detailed three-dimensional structure of  $\text{Li}_6\text{Zr}_2\text{O}_7$  is best described by first considering the zirconium oxide framework,

TABLE I  
REFINED ATOMIC PARAMETERS FOR  $\text{Li}_6\text{Zr}_2\text{O}_7$  WITH ESD'S IN PARENTHESES

Atom	Site	$x/a$	$y/b$	$z/c$	Occ.	$U_{\text{iso}}$ ( $\text{\AA}^2 \times 100$ )
X-ray $R_{\text{wp}} = 12.37\%$ , $R_{\text{ex}} = 4.80\%$ , $\chi^2 = 6.64$						
Neutron $R_{\text{wp}} = 8.38\%$ , $R_{\text{ex}} = 5.29\%$ , $\chi^2 = 2.51$						
Combined $R_{\text{wp}} = 10.76\%$ , $R_{\text{ex}} = 5.01\%$ , $\chi^2 = 4.60$						
$a = 10.4428(1)\text{\AA}$ , $b = 5.9877(1)\text{\AA}$ , $c = 10.2014(1)\text{\AA}$ , $\beta = 100.266(1)^\circ$						
Zr	8f	0.1833(1)	0.1223(2)	0.3642(1)	1.0(–)	1.37(3)
Li(1)	8f	0.2927(7)	0.1286(16)	0.1075(7)	1.0(–)	1.6(2)
Li(2)	8f	0.4341(7)	0.4030(18)	0.3980(7)	1.0(–)	1.2(2)
Li(3)	8f	0.0622(7)	0.3539(20)	0.0833(8)	1.0(–)	1.8(2)
O(1)	4e	0.0(–)	0.1467(9)	0.25(–)	1.0(–)	1.6(1)
O(2)	8f	0.1343(2)	0.3639(9)	0.5023(3)	1.0(–)	0.72(7)
O(3)	8f	0.3784(3)	0.3775(8)	0.0216(2)	1.0(–)	0.73(6)
O(4)	8f	0.2505(3)	0.3867(9)	0.2550(3)	1.0(–)	1.04(7)

TABLE II  
SELECTED CONTACT DISTANCES (Å) IN  $\text{Li}_6\text{Zr}_2\text{O}_7$ ,  
WITH ESD'S IN PARENTHESES

Zr-O(1)	2.061(1)
Zr-O(2)	2.144(4)
Zr-O(2')	2.137(3)
Zr-O(3)	2.047(4)
Zr-O(4)	2.125(5)
Zr-O(4')	2.061(4)
Li(1)-O(2)	2.16(1)
Li(1)-O(3)	2.02(1)
Li(1)-O(3')	2.02(1)
Li(1)-O(4)	2.26(1)
Li(1)-O(4')	2.12(1)
Li(2)-O(1)	2.29(1)
Li(2)-O(2)	2.09(1)
Li(2)-O(3)	1.99(1)
Li(2)-O(3')	1.98(1)
Li(2)-O(4)	2.19(1)
Li(3)-O(1)	2.29(1)
Li(3)-O(2)	2.08(1)
Li(3)-O(2')	2.08(1)
Li(1)-O(3)	1.92(1)
Li(1)-O(4)	2.40(1)

which may usefully be compared with that of ramsdellite ( $\gamma\text{-MnO}_2$ ). In ramsdellite,  $\text{MnO}_6$  octahedra share opposite edges to form columns; pairs of adjacent columns further edge-share to give double columns. In  $\text{Li}_6\text{Zr}_2\text{O}_7$  the  $\text{ZrO}_6$  octahedra are also arranged in these edge-sharing double columns but with alternate octahedra vacant,

leaving the  $\text{ZrO}_6$  octahedra isolated in edge-sharing pairs. The characteristic six-sided channel structure of ramsdellite is formed by corner-sharing between the double columns of octahedra. In  $\text{Li}_6\text{Zr}_2\text{O}_7$  similar six-sided channels also result from corner-sharing between the double columns and contain  $\text{Li}^+$  ions. The principal difference between the two structures lies in the nature of the oxygen packing and the resulting relationship between the double columns. The distorted hcp packing of ramsdellite results in two different orientations of the double octahedral columns with respect to the channels (Fig. 1a). This compares to the single orientation observed in  $\text{Li}_6\text{Zr}_2\text{O}_7$ , where a distorted ccp-based arrangement is preferred (Fig. 1b). Each  $\text{ZrO}_6$  octahedron shares one edge and three corners with neighbouring octahedra while one oxygen atom, O(3), does not bridge to other octahedra. The average Zr-O bond length of 2.10 Å is typical of octahedral zirconium in these systems and compares with an identical average in  $\text{Li}_2\text{ZrO}_3$  (6).

Three five coordinate  $\text{Li}^+$  ion sites can be identified in the structure (Fig. 2). All three  $\text{Li}^+$  ions adopt a square pyramidal geometry. The Li(1) ions are located above and below the Zr octahedra when projected onto the  $a/c$  plane and have four short bonds (2.02–2.16 Å) and one long (2.26

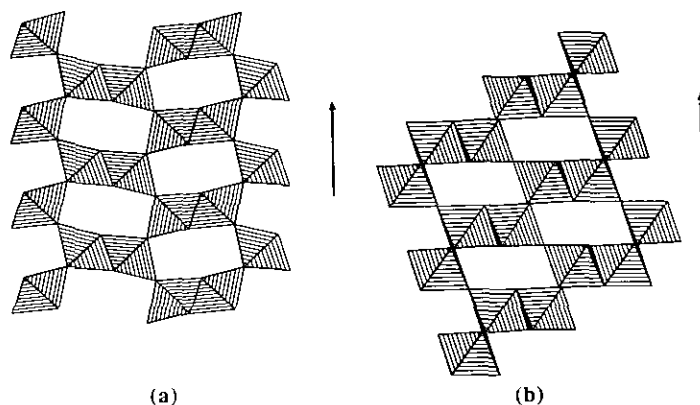


FIG. 1. Projection showing channel structure of (a) ramsdellite and (b)  $\text{Li}_6\text{Zr}_2\text{O}_7$ . Close packing directions are indicated by arrows.  $\text{Li}^+$  ions have been omitted from (b) for clarity.

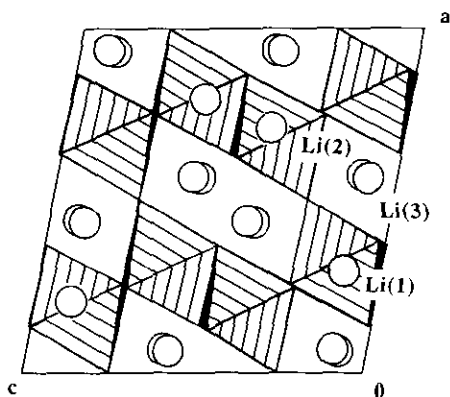


FIG. 2. Projection onto  $a/c$  cell plane of  $\text{Li}_6\text{Zr}_2\text{O}_7$ , with octahedra and open circles representing  $\text{ZrO}_6$  units and  $\text{Li}^+$  ions, respectively.

Å) bond to oxygen. Li(2) and Li(3) ions lie between the zirconium octahedra when projected onto  $a/c$ ; both have three short (1.92–2.09 Å) and two long bonds (2.19–2.40 Å) to oxygen, although in the case of Li(3) one of the long bonds is considerably longer than the other. Face sharing between polyhedra is avoided. The Li(1) and Li(2) sites both have four edge-sharing contacts to Zr octahedra and a further four to Li polyhedra. Li(3) differs in that it has only three shared edges with neighboring Zr octahedra, with five further edge sharing contacts to Li polyhedra. The arrangement of Li polyhedra is such that

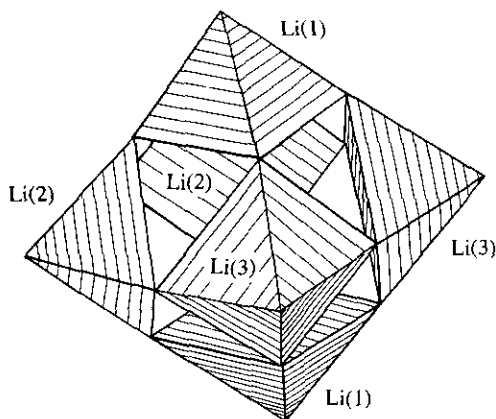


FIG. 3. Cluster of lithium square pyramids around oxide ion vacancy in  $\text{Li}_6\text{Zr}_2\text{O}_7$ .

they are clustered around the anion vacancies (Fig. 3). Since  $\text{Li}^+$  ions are located between the Zr octahedra in columns as well as within the channels formed by the columns,  $\text{Li}_6\text{Zr}_2\text{O}_7$  cannot be regarded as a true channel structure.

The fit to both data sets appears satisfactory as revealed in a plot of the difference profiles (Fig. 4). The use of the combined refinement results in a general improvement in esd's by a factor of 2–3, particularly for the Li and O positional parameters. This is explained not only by the increase in the number of observables but also by different contributions of Zr, Li, and O to the scattering of X-rays and neutrons. Use of the combined data therefore improves the refinement of the lighter atoms with respect to the heavier Zr, and also allows for a meaningful refinement of individual isotropic thermal parameters for all atoms.

The present study once again shows that relatively simple inorganic crystal structures can be determined in a straightforward manner from laboratory X-ray diffraction data. When data quality is very high, as in this case, even the positions of light atoms in the presence of a heavy scatterer can be deduced. This is in contrast to previous studies such as the structure determination and combined refinement of  $\text{BaBiO}_{2.5}$  (23) where the oxygen atoms were only unambiguously located after examination of the neutron data. The merits of a joint X-ray and neutron refinement can also be seen clearly in this work. Not only are the errors on refined structural parameters improved several times, but also successful refinement of individual isotropic thermal parameters has been possible. The structural parameters are in good agreement with the parallel single crystal X-ray study (24).

### Acknowledgments

We thank R. M. Ibberson at the Rutherford Appleton Laboratory for his assistance in data collection and the SERC for financial support. PGB gratefully acknowledges the Royal Society for a Pickering Research Fellowship.

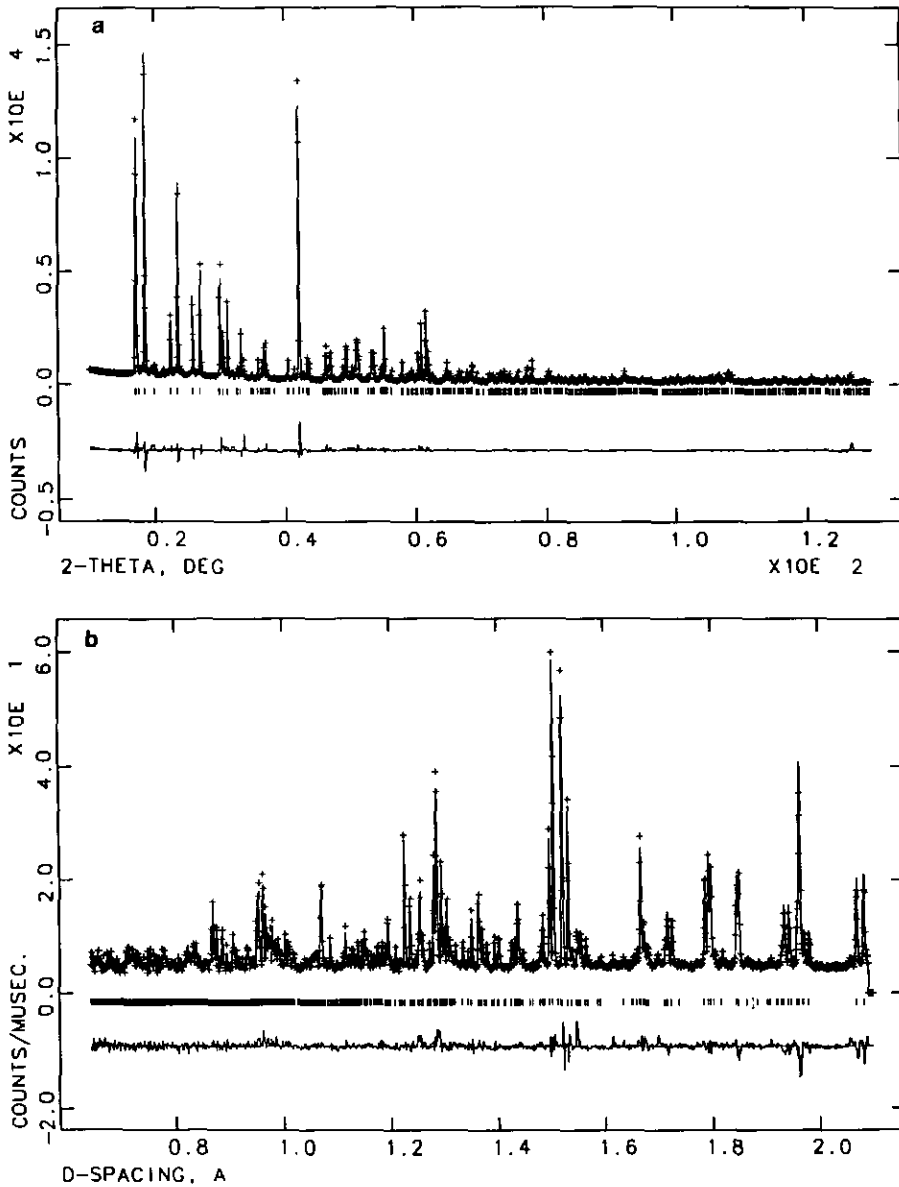


FIG. 4. Final difference profiles for  $\text{Li}_6\text{Zr}_7\text{O}_7$ ; (a) X-ray data and (b) neutron data. Observed (plus signs), calculated (lines), and difference (lower) profiles are shown with reflection positions indicated by markers.

## References

1. C. DELMAS, A. MAZAZ, F. GUILLEN, C. FOUASSIER, J. M. RÉAU, AND P. HAGENMULLER, *Mater. Res. Bull.* **14**, 619 (1979).
2. E. E. HELLSTROM AND W. VAN GOOL, *Solid State Ionics* **2**, 59 (1981).
3. D. J. SUITER, "Lithium Based Oxide Ceramics for Tritium Breeding Applications," Report MDC-E-2677, McDonnell Douglas Astronautics Co., St. Louis, MO (1983).
4. A. SKOKAN, in "Fusion Technology, 1990" (B. E. Keen, M. Huguet, and R. Hemsworth, Ed.), Elsevier, Amsterdam (1991).
5. H. KWAST, E. H. P. CORDFUNKE, AND R. MUIS in "Fabrication and Properties of Lithium Ceramics

- III" (I. J. Hastings and G. W. Hollenberg, Eds.), Amer. Chem. Soc., Washington, DC (1992).
6. J. L. HODEAU, M. MARZEIO, M. SANTORO, AND R. S. ROTH, *J. Solid State Chem.* **45**, 170 (1982).
  7. M. TRÖMEL AND J. HAUCK, *Z. Naturforsch. B* **23**, 110 (1968).
  8. H. A. LEHMANN AND P. ERZBERGER, *Z. Anorg. Allg. Chem.* **301**, 233 (1959).
  9. R. SCHOLDER, D. RÄDE, AND H. SCHWARZ, *Z. Anorg. Allg. Chem.* **362**, 149 (1968).
  10. A. NEUBERT AND D. GUGGI, *J. Chem. Thermodyn.* **10**, 297 (1978).
  11. L. J. ENRIQUEZ, P. QUINTANA, AND A. R. WEST, *Trans. Br. Ceram. Soc.* **81**, 17 (1982).
  12. JCPDS Card no. 20-645, Joint Committee on Powder Diffraction Standards, Swarthmore, PA (1976).
  13. JCPDS Card no. 34-312, Joint Committee on Powder Diffraction Standards, Swarthmore, PA (1976).
  14. G. P. WYRES AND E. H. P. CORDFUNKE, *J. Nucl. Mater.* **168**, 24 (1989).
  15. A. C. LARSON AND R. B. VON DREELE, Los Alamos National Laboratory Report No. LA-UR-86-748 (1987).
  16. W. I. F. DAVID, *J. Appl. Crystallogr.* **19**, 63 (1986).
  17. L. KOESTER AND H. RAUCH, Report 2517/RB, International Atomic Energy Agency (1981).
  18. "International Tables for X-ray Crystallography," Vol. IV, pp. 99-101 and 149-150, Reidel, Dordrecht (1974).
  19. R. X. FISCHER, *J. Appl. Crystallogr.* **18**, 258 (1985).
  20. W. D. S. MOTHERWELL, "PLUTO, Program for Plotting Molecular and Crystal Structure," Univ. of Cambridge (1976).
  21. P.-E. WERNER, "TREOR-4—Trial and Error Program for Indexing of Unknown Powder Patterns," Univ. of Stockholm (1984).
  22. A. LE BAIL, H. DUROY, AND J. L. FOURQUET, *Mater. Res. Bull.* **23**, 447 (1988).
  23. P. LIGHTFOOT, J. A. HRILJAC, S. PEI, Y. ZHENG, A. W. MITCHELL, D. R. RICHARDS, B. DABROWSKI, J. D. JORGENSEN, AND D. G. HINKS, *J. Solid State Chem.* **92**, 473 (1991).
  24. M. ZOCCHI, I. NATALI SORA, L. E. DEPERO AND R. S. ROTH, *J. Solid State Chem.* **104**, 391-396 (1993).